

Bending of an Elasto - Plastic Cracked Plate, Including the Effects of Crack Closure

D. P. Jones and J. L. Swedlow, Carnegie - Mellon University,
Pittsburgh, Pennsylvania, USA

We have considered the problem of a through crack centrally placed in a flat plate subject to a circular bending field. The plate is elasto-plastic in the sense described at the First International Conference [1]* and elsewhere (see, e.g., [2]). The geometry, loading, and material are depicted in Figures 1 and 2.

A theory permitting concurrent bending and stretching of the plate has been developed [3] based on a theorem analogous to that of Minimum Potential Energy. Since the neutral surface can shift as load accumulates, local unloading and reloading are necessarily incorporated into the theory, but with no Bauschinger effect. Boundary conditions are of the Kirchhoff type and are thereby not optimal for crack problems [4]; development of a higher order theory as used in [5] was deemed prohibitive. The theory admits the requirement of crack closure: we may treat the (no closure) case in which the material on the compression surface of the plate passes into itself, as is usually done in bending analyses, or we may limit crack surface motion to closure of the compression edges only. We have done both, and the latter case induces local stretching in addition to the bending field.

The theory has been implemented through the development of a finite element computer program whose main feature is that it avoids matrix inversion or reduction methods. Instead, the functional used to formulate the theory is minimized for each load step. That such a procedure is admissible follows from the quasi-linearity of the governing equations [2]. This approach is further advantageous in that the result of the n th step (suitably scaled) provides the initial estimate for the solution to the $(n+1)$ th step. The first (elastic) load step solution time is competitive with those for matrix reduction methods; subsequent steps are considerably faster.

Elastic Results: Deformed crack shapes appear in Figures 3 and 4 for the two cases, with and without closure. In the isometric sketches of Figure 3, the displacements are drawn to an exaggerated scale for clarity. As seen in Figure 4, the edges defined by the intersection of the crack face and the plate surfaces are symmetric in the no closure case. Closure, however, creates an asymmetry and a greater opening on the tension surface of the plate. The effect of closure is further evident in Figure 5 which shows contours of $\partial w / \partial y$, where w is transverse plate deflection. Figure 6 depicts positions of the neutral surface for several values of the coordinate x . (We define the neutral surface as the locus of points for which v , the displacement in the y -direction, vanishes.) The neutral surface is precisely on the plate's compression surface along the crack itself; it coincides with the mid-plane along the x -axis and far from the crack; and it is in transition in the vicinity of the crack. Note that the same result cannot be obtained by applying combined tension and bending far from the crack because the loads induced by crack closure vary along the crack.

*Numbers in brackets denote references listed at the end of the text.

Bending moments are shown along the x-axis in Figure 7 which shows this moment along the crack face induced by crack closure. Elastic stress variations through the plate's thickness are given in Figure 8 at $(x, y) = (3a/32, 0)$, and it is seen that closure also generates a compression ahead of the crack tip. The increases in opening of the crack (Figure 4) and stresses ahead of it (Figure 8) indicate an increase in the bending stress intensity factor K for cracks with closure taken into account. Using displacement data along the crack face, we estimate that taking closure into account elevates K by some 20% over the no-closure value on the tension surface of the plate.

Selected Elasto-Plastic Results: Yielding is first detected in the no-closure case at $M_0 = 267$ in-lb/in, and at 352 in-lb/in in the closure case. We show results for the greatest moment reached in both cases (724 in-lb/in), which is well into the plastic range for both problems. In the no-closure case, the yield zone (defined as that region in which τ_0 is beyond the linear portion of the curve) is symmetric about the mid-plane of the plate and has the shape shown in Figure 9. In the closure case, the tension surface is the site of first yield, and the zone grows inward. Then yield occurs on the compression surface and achieves the shape shown in Figure 10. Note the asymmetry in these shapes. Two further features of both cases are worthy of comment. First, the considerable growth of the yield zone along the crack is due largely to our use of Kirchhoff boundary conditions. It will be recalled from [4] that, although the equivalent shear force vanishes on the crack faces, the shear stress component does not. We expect that a higher order theory such as that in [5] would lead to zone shapes more nearly similar to those in [1]. Second, there is a sizeable elastic core so that, among other points, use of a strip model as in [6] may be an inappropriate model of this problem. It is interesting to observe further that, although the closure case generates higher stresses at the crack tip, it also leads to smaller yield zones. There is evidently more elastic constraint and, in addition, the closure case produces a stiffer plate. That is, for a given remote loading, less plate deflection occurs and less plastic strain can accrue.

A related effect is observed in the opening of the crack at peak load. We show in Figure 11 the relatively greater blunting for the no-closure case as normalized on the elastic shapes: It may again be inferred that little plastic straining occurs in the closure case. In the early stages of yield, the neutral surface in the closure case shifts from the position shown in Figure 6 closer to the compression surface of the plate. As the compressive yield zone develops, however, the elastic core becomes thinner, and the neutral surface moves back toward the mid-plane. Then an increasing portion of the load is carried by the elastic core, whose significance becomes more evident.

The originally linear (with z) stress distribution becomes non-linear as shown in Figure 12; the effects of both yield and closure are clear. Stresses at several positions ahead of the crack tip vary with load as shown in Figure 13. The peaking and subsequent reduction reported earlier [1] are evident, and much of that discussion applies here as well.

Further Remarks: We have shown briefly the main findings of this study, and note that extensive detail appears in [3]. Even with the use of Kirchhoff boundary conditions, it is clear that the effects of elasto-plastic flow and crack closure are significant in the mechanics of the response of a cracked plate to a circular bending moment in the far field. These effects are seen in opening of the crack, location of the neutral surface, calibration of the bending stress intensity, and growth of yield zones. We observe further that $\partial w / \partial y$ is a sensitive indicator of the closure phenomenon, a point that may prove useful in designing experiments for further research.

Acknowledgements: One of us (DPJ) acknowledges Westinghouse Bettis Atomic Power Laboratory for granting a leave of absence in order to complete this work.

References:

1. M. L. Williams, J. L. Swedlow, and W. H. Yang, *Proc 1st Int Conf on Fract 1* (1966) 259-282.
2. J. L. Swedlow, *Int J Non-Linear Mech* 3 (1968) 325-336; 4 (1969) 77.
3. D. P. Jones, Report SM-83, Dept of Mech Engrg, Carnegie-Mellon University (1972).
4. M. L. Williams, *J of Appl Mech* 28 (1961) 78-82.
5. J. K. Knowles and N. M. Wang, *J Math Phys* 39 (1960) 223-236.
6. H. F. Brinson and H. Gonzales, Report VPI-E-71-11, College of Engineering, Virginia Polytechnic Institute and State University (1971).

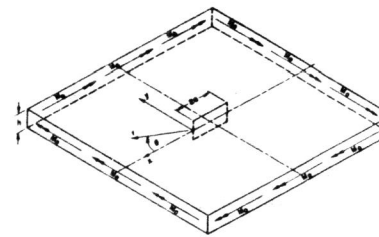


Fig 1, Geometry and Loading

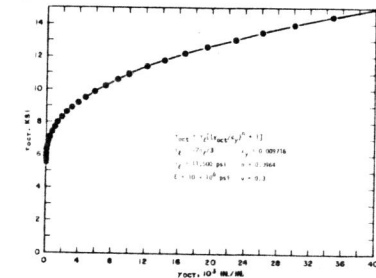


Fig 2, Stress-Plastic Strain Curve

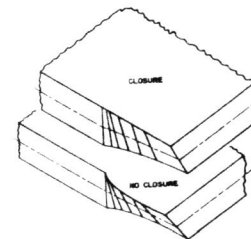


Fig 3, Elastically Deformed Crack Faces

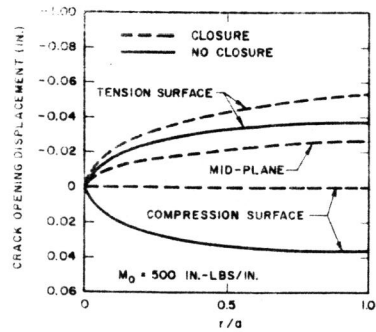


Fig 4, Elastic Crack Opening Contours

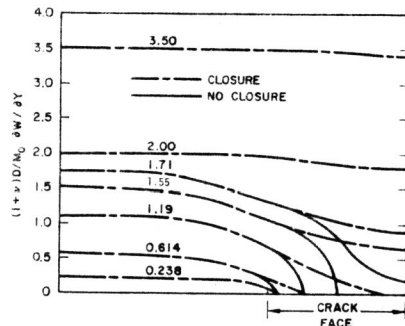


Fig 5, Elastic Contours of $\frac{dw}{dy}$

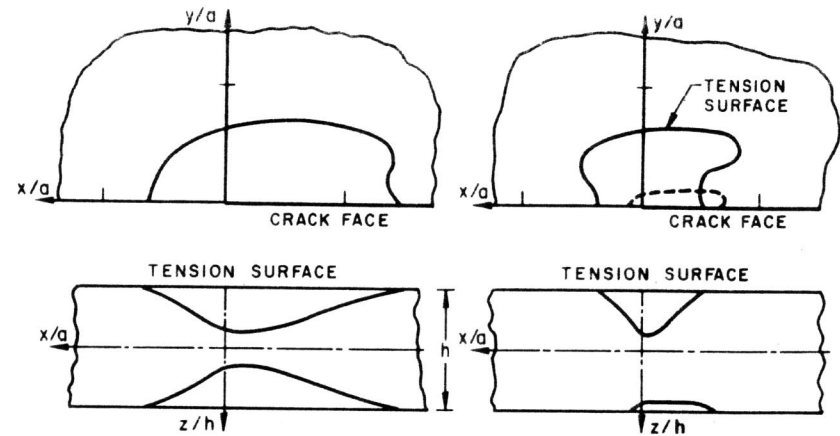


Fig 9, No-Closure Yield Zones

Fig 10, Closure Yield Zones

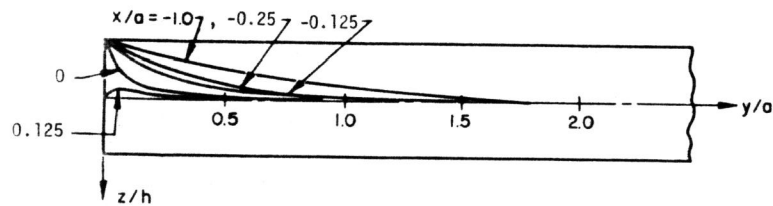


Fig 6, Shift of Neutral Surface

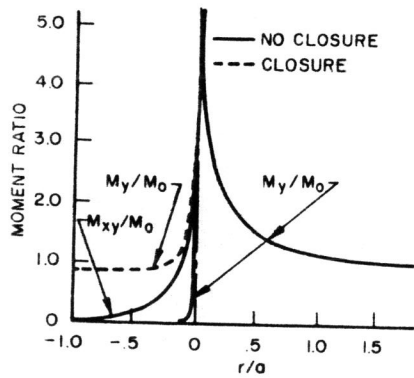


Fig 7, Elastic Moment Distribution

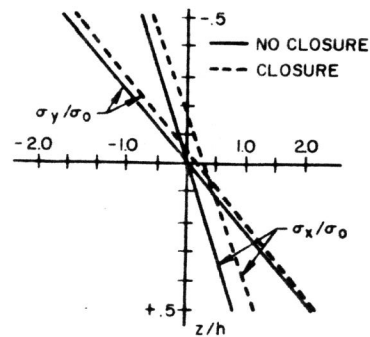


Fig 8, Elastic Stresses ahead of Crack Tip

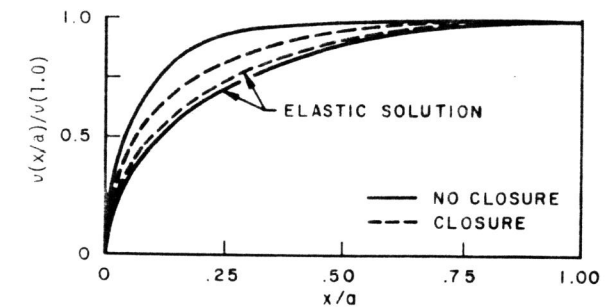


Fig 11, Crack Blunting with Elasto-Plastic Flow

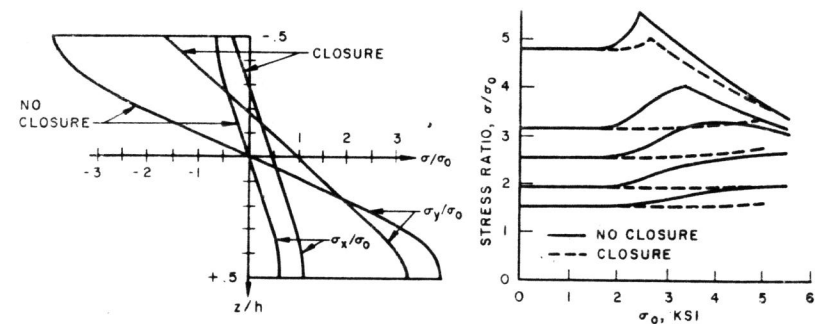


Fig 12, Elasto-Plastic Stresses ahead of Crack Tip

Fig 13, Stress Redistribution